A THEORETICAL EXAMINATION OF GROWTH AND MORTALITY TRADEOFFS ON POPULATION GROWTH RATE AND SIZE STRUCTURE

by

ELISE KAM YUK KRUEGER

(Under the Direction of Ford Ballantyne IV)

ABSTRACT

A stage-structured discrete time model was used to examine how size-specific tradeoffs between biomass accumulation and predation risk are influenced by changes in reproductive mode in a theoretical population. The size class with the largest aggregate growth rate, the product of the biomass accumulation rate and probability of survival, was found to be an absorbing class such that any reproductive strategy combined with a specified tradeoff which yields a larger proportion of individuals of the dominant size class should be favored. This model suggests that the steepness of the selection gradient for this reproductive mode becomes increasingly shallow when populations exhibit frequent switching between size classes. This model also suggests that selection gradients may become steeper or shallower depending on changes in the nutrient or predation environment.

INDEX WORDS: Ecological modeling, Discrete time model, Population growth, Tradeoffs, Predation

A THEORETICAL EXAMINATION OF GROWTH AND MORTALITY TRADEOFFS ON POPULATION GROWTH RATE AND SIZE STRUCTURE

by

ELISE KAM YUK KRUEGER

BA, New York University, 2004

A Thesis Submitted to the Graduate Faculty of The University of Georgia in Partial Fulfillment of the Requirements for the Degree

MASTER OF SCIENCE

ATHENS, GEORGIA

2018

A THEORETICAL EXAMINATION OF GROWTH AND MORTALITY TRADEOFFS ON POPULATION GROWTH RATE AND SIZE STRUCTURE

by

ELISE KAM YUK KRUEGER

Major Professor:	Ford Ballantyne IV
Committee:	John Drake
	Ricardo Holdo

Electronic Version Approved:

Suzanne Barbour
Dean of the Graduate School
The University of Georgia
August 2018

ACKNOWLEDGEMENTS

I would like to express thanks to my committee members throughout my graduate career: Richard Shefferson, Nina Wurzburger, Brian Hopkinson, John Drake, Ricardo Holdo, and Ford Ballantyne IV, for providing me guidance throughout this process. I would also like to acknowledge the contributions of both Chao Song and John Vinson who served as sounding boards for my ideas and provided considerable assistance with both computation and programming.

TABLE OF CONTENTS

Page

LIST OF TABLES

Page

LIST OF FIGURES

Page

CHAPTER 1

INTRODUCTION

Virtually all organisms exhibit some degree of plasticity in body size, both over an individual's lifetime and across individuals within a population. Variation in body size affects life history by influencing time to reproduction (Cuadrado & Loman, 1999), the number of offspring produced (Cole, 1954), or the ability to disperse (Jenkins, et al., 2007). Body size may also alter an organism's ability to obtain necessary resources, for example by reducing or increasing rates of nutrient or prey acquisition (Eppley & Thomas, 1969; Hein, et al., 1995). The distribution of body sizes within a population may also affect how that population interacts with other organisms and the surrounding habitat (Bassar, et al., 2010). Variation in body size is acknowledged to have dramatic effects on community composition (Hutchinson, 1959), food web structure (Brooks & Dodson, 1965), and ecosystem productivity (Ryther, 1969). While an understanding of these large-scale effects is important, there is still a need to better identify how, and why, populations vary in size structure and what processes may be driving and driven by organism size. Because evolution strongly influences body size (Roughgarden & Fuentes, 1977; Charnov, 1993; Charnov, 1991), focusing on the selection pressures influencing body size is therefore key for achieving a better understanding of body size evolution and its consequences for higher level ecological interactions and dynamics.

One prominent driver of changing body sizes is size-selective predation, which has been shown to drive not only plastic changes in morphology but has also been identified as a likely driver for the Precambrian evolution of multicellularity (Stanley, 1973; Boraas, et al., 1998;

Ratcliff, et al., 2012). It has been hypothesized that early ecosystems consisted largely of producers and exhibited limited taxonomic and morphological diversity. The evolution of phagotrophy reduced resource limitation, allowing increased competition and morphological diversity within preexisting organisms, leading to the eventual evolution of multicellular body forms (Stanley, 1973). This dynamic has been recreated experimentally using the alga *Chlorella vulgaris* and the protist *Ochromonas vallescia*. Introduction of *O. vallescia* into a laboratory population of unicellular *Chlorella* resulted in oscillating predator-prey abundance (Boraas, et al., 1998). During each subsequent prey recovery period multicellular clusters of *Chlorella* made up an increasingly large proportion of the population, providing evidence that predation is a potential driver for multicellular development (Boraas, et al., 1998).

To better understand what is driving morphological shifts in body size one must consider how physiology and ecological interactions influence survival and reproduction. For many organisms, predator-prey interactions are size dependent so that the likelihood of being consumed is higher or lower depending on an individual's size relative to other individuals or prey items (Brooks & Dodson, 1965; Pastorok, 1981; Arnold, 1984; Sala & Zabala, 1996). For many organisms, increased size increases visibility to predators so that larger individuals are more susceptible to predation, which results in a decrease in mean body size of the population (Reznick & Endler, 1982). In many aquatic systems the primary herbivores are filter feeders, such as rotifers or daphnia, and because ingestion by filter feeders is largely limited by particle size, being larger decreases an individual's chance of being consumed. Even when predators more actively pursue prey, larger prey may have greater survivorship as predators must expend more energy to pursue, handle, and consume larger organisms (Pastorok, 1981; Sala & Zabala, 1996; Nilsson & Bronmark, 2000; Pawar, et al., 2012). Conversely, if predators target small

organisms, due for example to gape limitation, prey will be less susceptible to predation as they grow larger. Growing larger may not pose significant challenges for many organisms but unicellular organisms can only grow so big before reaching the limits of metabolic efficiency (Kempes, et al., 2012), thus the selection for increased size to avoid predation is constrained by increasing metabolic demands (Yoshida, et al., 2003).

Because there are a wide range of potential size-related responses, one way to examine size is to consider size in the context of unicellular and multicellular body forms. Cell number may be used as a proxy for increased size as this model accounts for cell biomass and assumes that the minimum size of a multicellular individual is always greater than the maximum possible size of a unicellular individual. Functionally, within this model increasing the number of cells is equivalent to increasing size. As cell size increases, volume increases more rapidly than surface area, thus slowing the rate of nutrient accumulation and distribution per unit volume throughout the cell, and by extension lowering the cell's growth rate (Eppley & Thomas, 1969; Hein, et al., 1995; Irwin, et al., 2006). This general pattern holds not only as individual cells get larger, but also as multicellular clusters increase in size. Because smaller cells have an advantage in terms of nutrient acquisition, distribution, and utilization, these cells may also have a potential fitness advantage. For instance, if reproduction requires a doubling of initial biomass, it will take less time for smaller cells to accrue the necessary biomass for reproduction; this would allow for earlier and more frequent reproductive events.

The need to mitigate multiple ecological stressors means many organisms exhibit plastic and adaptive responds in relation to environmental pressures and interactions with other organisms. These responses may include changes in behavior, morphology, or physiology and may result in altered life history strategies to reduce susceptibility to predation or increase rates

of biomass accumulation. The green alga *Chlamydomonas reinhardtii* has been used as a model organism to examine both plastic and evolutionary responses to the tradeoff between growth and predation risk (Ellner & Becks, 2011; Lurling & Beekman, 2006; Becks, et al., 2010; Fischer, et al., 2014). *Chlamydomonas* may be characterized by multiple morphological forms ranging from a unicellular flagellated individual to multicellular palmelloid clusters. Under low predation and high nutrient conditions the unicellular morphology dominates. However, environmental and ecological stressors, such as increases in predator density or the presence of environmental toxins, are known to induce a change to a multicellular morphology (Iwasa & Murakami, 1968; Lurling & Beekman, 2006; Ratcliff, et al., 2012). This drastic morphological change implies over multiple generations organisms that exhibit this response will have a significant fitness advantage over organisms that do not.

CHAPTER 2

A SIZE STRUCTURED MODEL INCORPORATING TRADEOFFS BETWEEN GROWTH AND MORTALITY

If increased size reduces mortality but decreases individual growth rates, which for the purposes of this model is the biomass accumulation rate, the consequences of potential tradeoffs between growth and mortality in a theoretical population can be examined to determine how these tradeoffs alter population growth rates and the selection for unicellular or multicellular morphology. To address the consequences of a tradeoff between growth and mortality as a function of size, I consider how a single species' reproductive mode may be modified to maximize the asymptotic population growth rate. I assume an ancestral unicellular morphology, but allow the organism to develop a multicellular morphology, which is analogous to the morphological plasticity exhibited by *C. reinhardtii* and other species of *Volvocene* algae where both morphological forms may be present within the same population (Michod, 2005). For the purposes of this model, larger cells have twice as much biomass as small cells, which may be thought of as conceptually the same as a two-cell cluster, which maintains a relatively spherical shape (Figure 1). Reproduction in this system occurs through fission and can only occur after a doubling of an individual's biomass regardless of form. Mortality in this system is largely dictated by the environment, specifically the density of predators.

To account for the morphologically distinct size classes, I developed a simple stage structured model to describe the population dynamics (Caswell, 2001).

$$A = \begin{bmatrix} r_1(1-g)(1-m_1) & \rho(1-m_2) \\ g(1-m_1) & r_2(1-\rho)(1-m_2) \end{bmatrix} \quad (1)$$

In this model, g represents a life history branchpoint where, after a doubling in biomass, a unicell may reproduce as unicells or become multicellular. An additional branchpoint is represented by ρ, which determines whether multicellular individuals remain colonial upon reproduction or revert to the ancestral unicellular morphology (Figure 1). The r_i terms denote the growth rates, in terms of biomass accumulation (mass per unit time) and m_i represents the class-specific probability of mortality per unit time.

For any situation, I assume that *r* and *m* are fixed by the organism's size and its environment, influenced by resource availability and predator density respectively. The aggregated population growth rate for either class is given by:

$$R_i = r_i(1 - m_i) \quad (2)$$

where R_i indicates the combined effect of growth and survivorship on a given class. When $R_i > 1$ for any class I expect that class to be growing, if $R_i < 1$ the class exhibits a growth decline. The ability to transition between classes creates the potential for reproductive cycles. For example, if individuals always begin in the unicellular class but must pass through the multicellular class before being reproductively viable then cycles may arise as individuals in a cohort all reach reproductive capability at approximately the same time giving rise to a new generation of individuals which will follow a similar reproductive schedule (deRoos & Persson, 2013).

I will consider how a tradeoff between predation defense and nutrient acquisition alters not only R_i but also the population's size structure and long-term asymptotic growth rate (λ). I assume that growth and mortality rates are always greater for the unicellular size class; this allows me to characterize the reduction in growth and mortality with increased size using the following set of equations.

$$r_2 = r_1 - b \quad (3)$$

and

$$m_2 = m_1 - c \tag{4}$$

Following from this I describe the aggregate growth rate for uni- and multicellular classes as:

$$R_1 = r_1(1 - m_1) \tag{5}$$

$$R_2 = (r_1 - b)\big(1 - (m_1 - c)\big) \tag{6}$$

Here *b* and *c* represent the decreases in vital rates from unicellular to multicellular size classes. As the specific tradeoff between growth and mortality is defined by the combination of *b* and c values it is now possible to evaluate several possible tradeoffs.

When $R_1 = R_2$ the aggregate growth for each class is identical and neither class exhibits a growth advantage. The range of tradeoffs, combinations of *b* and *c*, that correspond to this neutral condition can be parameterized as

$$b = T(c) = r_1 - \frac{r_1(1 - m_1)}{1 - (m_1 - c)} \tag{7}$$

Figure 2 shows the shape of the neutral tradeoff for different values of unicellular mortality. When unicellular mortality is low ($m_1 = 0.2$), *b* and *c* exhibit change at approximately the same rate indicating a near-parallel decrease in biomass accumulation and predation rates will maintain the neutral tradeoff. As mortality increases the shape of the tradeoff becomes increasingly curved and decreasing mortality, indicated by the larger values of *c*, becomes more influential to maintain this neutral tradeoff. If $R_1 = R_2$, then a mixed population of uni- and multicellular individuals is the expectation because size differences have no effect on fitness or the long-term population growth rate and the maximum population growth rate may be achieved with any proportion of morphologies. By varying *b* and *c*, the tradeoff between growth and mortality changes resulting in a change in the relationship between R_1 and R_2.

As noted above, organisms frequently require a threshold biomass, or size, before they are physiologically able to reproduce or transition between classes. To account for this, I modified the projection matrix to incorporate time between branching point events using pseudoclasses (Caswell, 2001). Pseudoclasses essentially function as a way of slowing down individual movement through the model; this also allows me to partially accommodate a continuous process in a discrete time model. I employ pseudoclasses here in order to prevent reproduction or transition into the next class before the necessary amount of biomass is accrued. The number of pseudoclasses is defined by R_i and may vary for each size class, however all pseudoclasses within a class are considered to have equal rates of growth and mortality (Caswell, 2001). To conveniently define the appropriately sized projection matrix for aggregate class growth rates, R_i, I use roots of two to define R_i. Using roots of two results in an integer number of pseudoclasses for any R_i and is merely for mathematical convenience. For example, if $R_i = \sqrt{2}$ then it will take two timesteps for biomass to double; slower growth rates are defined by increasing the n^{th} root. The projection matrix below (Equation 8) is defined by $R_1 = \sqrt{2}$ and $R_2 = \sqrt[3]{2}$. Thus, it takes two timesteps for a unicell individual to reach the threshold size for a potential morphological switch, whereas it will take a multicell individual three timesteps to accumulate enough biomass to reach the required threshold for division.

$$A = \begin{bmatrix} r_1(1-g)(1-m_1) & 0 & 0 & 0 & r_2(1-m_2) \\ r_1 g(1-m_1) & 0 & 0 & 0 & 0 \\ 0 & r_1(1-m_1) & r_2(1-\rho)(1-m_2) & 0 & 0 \\ 0 & 0 & r_2\rho(1-m_2) & 0 & 0 \\ 0 & 0 & 0 & r_2(1-m_2) & 0 \end{bmatrix} \quad (8)$$

Table 1: Model Parameters

	Parameter	Range
$\boldsymbol{r_i}$	biomass accumulation rate, mass per unit time	0-1
$\boldsymbol{m_i}$	probability of mortality per unit time.	0-1
$\boldsymbol{g}$	probability of transition from unicellular to multicellular	0-1
$\boldsymbol{\rho}$	probability of transition from multicellular to unicellular	0-1
$\boldsymbol{b}$	difference in biomass accumulation rate from unicellular to multicellular	0-r_1
$\boldsymbol{c}$	difference in mortality from unicellular to multicellular	0-m_1

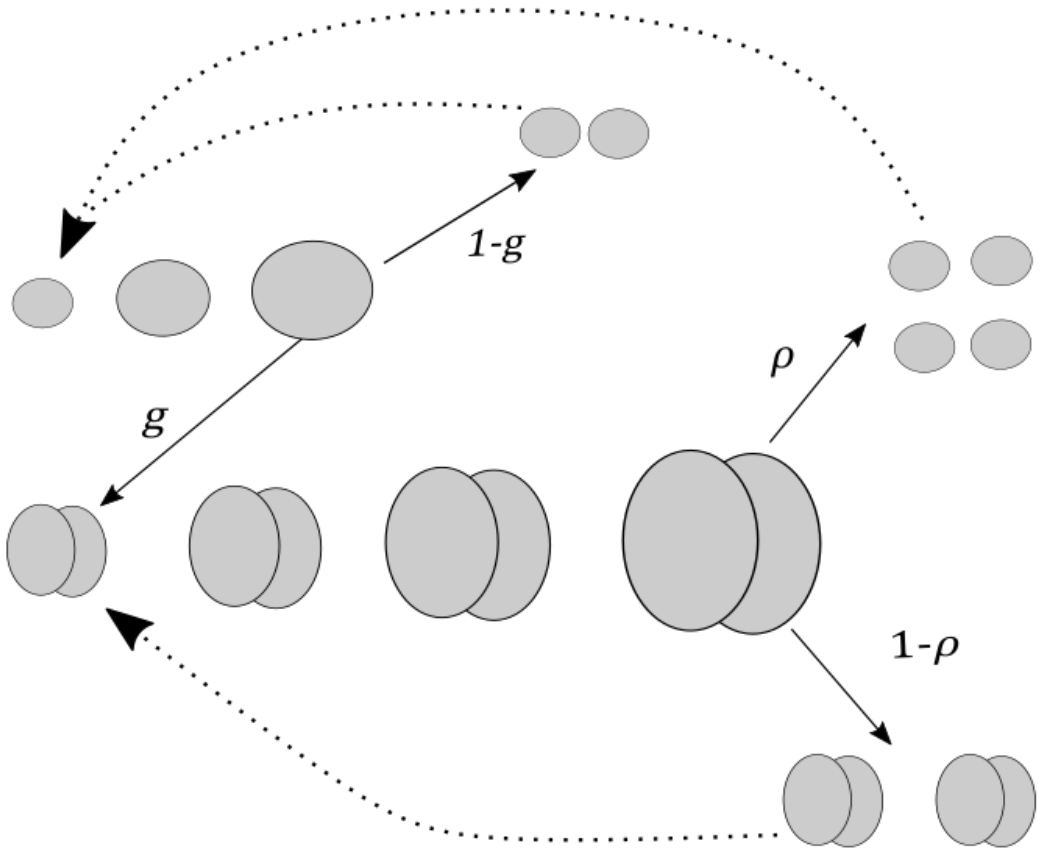

Figure 1: Potential life history pathways represented by the projection matrix. A unicell grows until it reaches the first branching point, *g*. Here the unicell may split into two separate unicells (*1-g*) or may become multicellular (*g*). A multicell individual continues to grow until it reaches a second life history branching point representing two reproductive paths. The multicell may reproduce into the ancestral unicellular morphology (ρ) or the multicellular morphology may persist ($1-\rho$).

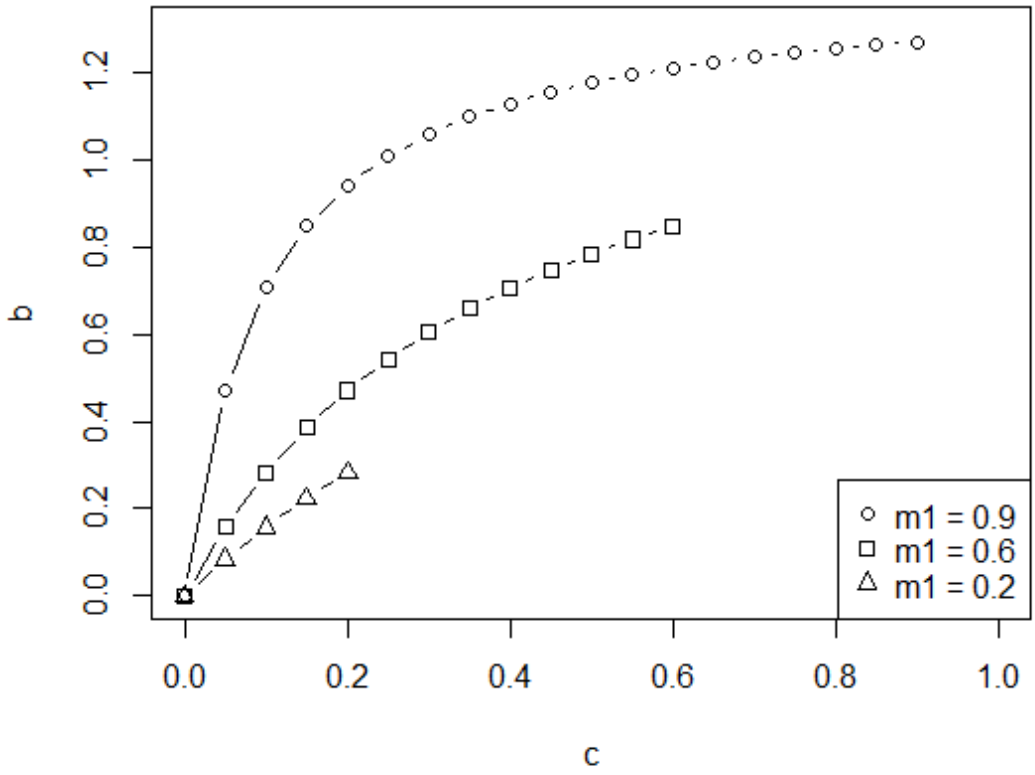

Figure 2: The shape of $T(c) = b$ under three different mortality scenarios. The value of m_1 was altered to examine high, medium, and low levels of mortality. Increasing unicellular mortality increases the range of possible c values. Here r_1 is held constant. and the value of m_2 is varied to specify the c value, with larger differences in m_1 and m_2 increasing c.

CHAPTER 3

ANALYSIS OF THE MODEL

Tradeoffs representing deviations from the neutral case presented above are achieved through differing combinations of *b* and *c* so that class-specific biomass accumulation and mortality rates fall either above or below the neutrality curves in Figure 2. I first computed population growth rates by holding the class-specific growth rates, r_1 and r_2, constant while cycling through all combinations of g and ρ for all possible mortality combinations for both cell classes (Figure 3); this analysis holds *b* constant while allowing *c* to vary. Holding the r_i values constant is akin to evaluating the influence of life history variation, changing g and ρ, under a given but constant nutrient environment. I varied g and ρ from zero to one in increments of 0.05. When either is zero, individuals, and their associated biomass, always remain in their initial class, whereas a value of one for either class means that individuals always transition into the other morphology. Mortality for each class varies between zero and one.

For each combination of g, ρ, and class-specific mortality parameters, m_1 and m_2, the *eigen* function in R (version 3.3.2) was used to determine the eigenvalues and eigenvectors of the projection matrix. The asymptotic population growth rate was determined by the dominant eigenvalue. The stable class distribution showing the proportion of unicellular and multicellular individuals in the population is determined from the eigenvector associated with the dominant eigenvalue for each mortality combination (Figure 4). The proportion of unicells was determined by finding the proportion of all individuals within the unicellular pseudoclasses. The contours in Figure 3 are L-shaped and the corners are shifted downward from the 1:1 for mortality. This is

due to the assumption that $r_2 < r_1$ so that the aggregate growth rate for multicellular individuals will always be less than the aggregate growth rate for unicells when mortality is equal for both classes.

As with the population growth rates, morphological dominance does not fall directly on the 1:1 mortality line, this is again a consequence of the unicellular growth advantage, especially when unicell mortality is low. This makes intuitive sense given the definitions above, when mortality is low for unicells it will also be low for multicells, indicating that at low mortality the influence of growth becomes greater; multicells will never be able to reach a growth rate equivalent to unicells because of the stipulation that $r_2 < r_1$. As unicell mortality rises, the proportion of multicell individuals in the population increases drastically, and only increasingly high rates of multicell mortality favors unicellular dominance. The trends between the population's maximum growth rate and the dominant morphologies are not surprising as these findings are largely a consequence of the model and its assumptions. Next, I examine how altering the tradeoffs between growth and mortality change patterns in population growth rate and structure.

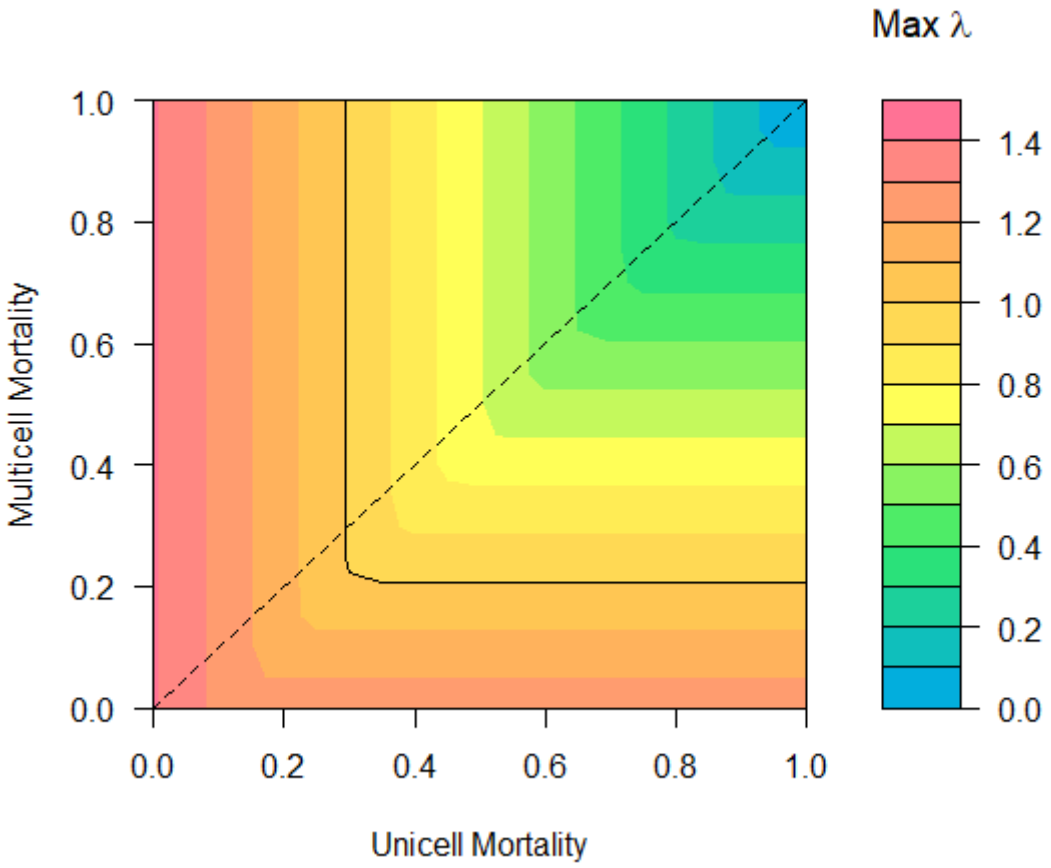

Figure 3: Asymptotic population growth rate (λ) of a theoretical population across all mortality rates. All values of g and ρ were evaluated for each mortality combination and the maximum dominant eigenvalue for each mortality combination is presented in this figure. Warmer colors indicate a greater maximum lambda value. The dashed line indicates equivalent mortality for the two classes. The solid line indicates the contour where $\lambda = 1$. Above this line the population is declining, below this line the population shows growth. When mortality for both classes is high, the asymptotic growth rate is low. Given the definition of mortality in the theoretical population, multicell mortality cannot exceed unicell mortality, therefore the primary region of interest lies below the 1:1 line.

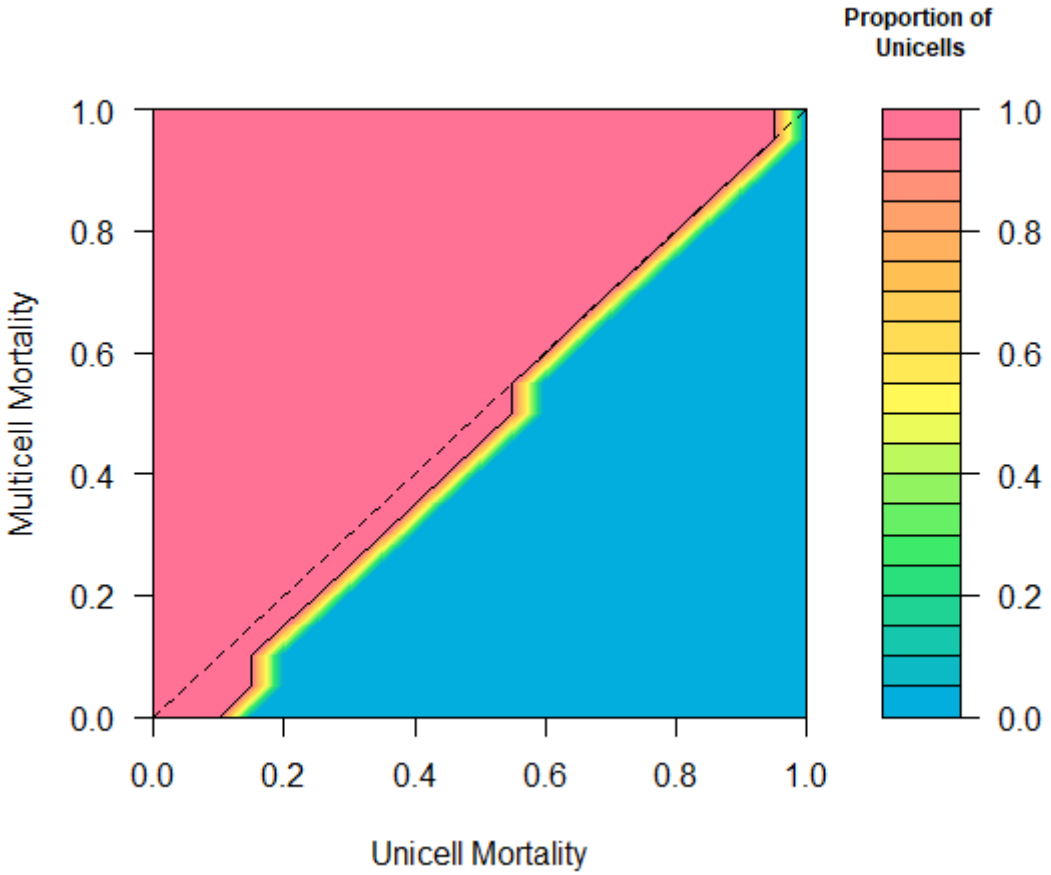

Figure 4: The proportion of unicells present in the theoretical population across all combinations of mortality. These proportions correspond to the maximum dominant eigenvalue for each mortality combination across all values of g and ρ (as presented in Figure 3). Warmer colors represent a greater proportion of unicells in the population, and cooler colors a greater proportion of multicell individuals. The dashed line shows 1:1 mortality. The solid line indicates where the proportion of unicells = 1, so that above this line the population consists only of unicellular individuals. Warmer colors indicate greater proportions of unicells.

CHAPTER 4

CONSEQUENCES OF TRADEOFFS ON POPULATION GROWTH AND SIZE STRUCTURE

The initial analysis of the model masks the effect of reproductive mode on the tradeoffs between growth and mortality on population growth and size structure. From Figures 3 and 4 it cannot be determined which life history strategies correspond to a specific growth rate or morphological distribution. In contrast to computing the maximum growth rate and associated size structure across all life history strategies, I now explicitly relate life history transitions to population growth and size structure for two tradeoffs that differ from neutrality. Neutrality in this system occurs when $R_1 = R_2$, so that neither class exhibits a competitive advantage (Figure 2, Equation 7). I first identified all g and ρ values associated with the maximum λ for each mortality combination. The patterns presented in Figures 5 and 6 resembles the pattern of morphological distribution of unicells and multicells (Figure 4); equivalent mortality defines the approximate areas where there is a switch in the influence of g and ρ. When multicell mortality is higher than unicellular mortality only a single g value, $g = 0$, is associated with the maximum population growth rate. When unicellular mortality is higher than multicellular mortality any value of g may be associated with the maximum growth rate. If there is a non-zero chance of becoming multicellular all lineages will eventually make the transition to multicellularity; ρ will be zero in this case and the multicellular morphology is an absorbing state. Similarly, in the parameter spaces where $g = 0$, all values of ρ may yield the maximum population growth rate as the unicellular class is now the absorbing state. This provides additional confirmation that the

highest population growth rate will be attained by a monomorphic population consisting of the morph with the highest R_i.

To examine how tradeoffs in growth and mortality work in conjunction with changes in reproductive life history to alter growth dynamics and size structure, I modified the projection matrix to correspond to tradeoffs that deviate from the neutral case presented above; this allows for two scenarios $R_1 > R_2$ and $R_1 < R_2$. Because g and ρ define the potential life history pathways, the model was parametrized to calculate each tradeoff scenario for each g and ρ combination thereby determining both the largest maximum lambda and the proportion of unicellular individuals associated with that lambda value.

To assess the first tradeoff scenario ($R_1 < R_2$) I started by defining the aggregate class growth rates, unicellular mortality, and using Equations 2 – 6 to determine the additional growth and mortality rates for our model. Aggregate class growth rates were defined as $R_1 = \sqrt{2}$ and $R_2 = \sqrt[3]{2}$. The biomass accumulation rates under this tradeoff are $r_1 = 2$ and $r_2 = 1.65$. Mortality was defined as $m_1 = 0.2928932$ and $m_2 = 0.2364115$ representing a relatively low predator density. For all values of g and ρ, $\lambda > 1$, with the highest possible growth rate being $\lambda = \sqrt{2}$ while the lowest growth rate is $\lambda = \sqrt[3]{2}$. These values correspond to the aggregate growth rates for our two classes, with intermediate asymptotic growth rates falling between R_2 and R_1 (Figure 7).

Here, the largest population growth rate occurs when $g = 0$, meaning that no unicellular individuals should enter the multicellular class as the aggregate growth rate for unicells is equivalent to the maximum population growth rate. The lowest growth rates occur when $\rho = 0$, except when g is very low. As values of ρ increase, for any given g, the proportion of individuals returning to the unicellular morphology increases, resulting in a higher maximum population growth rate. When ρ is large, large decreases in g are required increase the population growth

rate. As values of ρ get smaller, minor decreases in g result in more rapid increases in growth rate, this is because unicellular individuals are less likely to make the transition to the multicellular form.

Population-specific life history strategies may be described by the initial vales of g and ρ. When g and ρ are small, organisms will tend to maintain the current morphology as the probability of transition into the alternate class is low. In contrast, organisms associated with high g and ρ values will exhibit a more itinerant life history with frequent movement between the two classes. Organisms in the off-diagonals, which have a large g corresponding to a small ρ, or vice versa, will be reluctant movers, such that they will generally remain within a specific class. For example, when, g is greater than ρ, the probability of transitioning from unicellular to multicellular is high, meaning that organisms should frequently transfer into the multicellular class, and due to the low ρ should rarely transfer out of this size class.

Under the current scenario, $R_1 > R_2$, the value of ρ is the biggest determinant of the population growth rate. When ρ is large, decreasing g increases the population growth rate, so there is a selection for a reduction in g. When g is large, there is a higher probability of branching into the multicellular class, the population growth rate is low driving selection for an increase in ρ. Because mortality between the two size classes is minimal, these trends indicate that the penalty of decreased growth for multicellular individuals outweighs the benefit of reduced susceptibility to predation.

Figure 8 illustrates the proportion of unicells associated with the maximum growth rate for each g and ρ combination when $R_1 > R_2$. Multicell individuals make up 50% or more of the population over much of parameter space. Looking at Figures 7 and 8 in conjunction, if selection is maximizing the asymptotic growth rate then there will be selection for increasingly low values

of g and the eventual replacement of all multicells with unicells. This reinforces the trends from Figure 7, where it was shown that the multicellular class exhibited a lower class-specific growth rate and that smaller values of g, should be selected for in the long term.

I now analyze the alternate case when $R_1 < R_2$. The simplest way to accomplish this is to swap the aggregate growth rates so that $R_1 = \sqrt[3]{2}$ and $R_2 = \sqrt{2}$. Unicellular mortality remained the same in this scenario, $m_1 = 0.2$ (Figure 9). The maximum and minimum asymptotic growth rates again correspond to the individual class growth rates, however in this case the maximum possible value, $\lambda = \sqrt{2}$, is now associated with R_2 and the minimum value is equivalent to R_1, $\lambda = \sqrt[3]{2}$. As the unicellular class now exhibits a lower growth rate, the projections are largely the inverse of the previous case. If selection increases the overall population growth rate, ρ will be reduced so that organisms which branch into the multicellular class will remain multicellular upon reproduction. Unicellular individuals will eventually all transition to multicellularity and will not be present in subsequent generations. Starting in the upper left, where unicellular organisms tend to remain unicellular while multicellular organisms return to unicellularity with high frequency, increasingly large values of g should be selected for as this will allow the population to increase the overall growth rate more rapidly; this results in an increasingly itinerant life history strategy. Large increases in g are required to achieve the same increase in growth rate when ρ is large. When g is large, larger reductions in ρ are required to increase the growth rate than when g is small.

I can examine the relative steepness of the selection gradient associated with a population that reaches a completely unicellular morphology when this form is associated with the maximum possible population growth rate. If I begin with a population where $g = 0.2$ and $\rho = 0$ and allow both parameters to evolve in steps of 0.05 in either g or ρ, the selection gradient to

reach the maximum possible population growth rate and exhibit a completely unicellular form is steeper than for populations starting with larger initial values of g (Figure 11). Increasingly large values of g will exhibit shallower selection gradients.

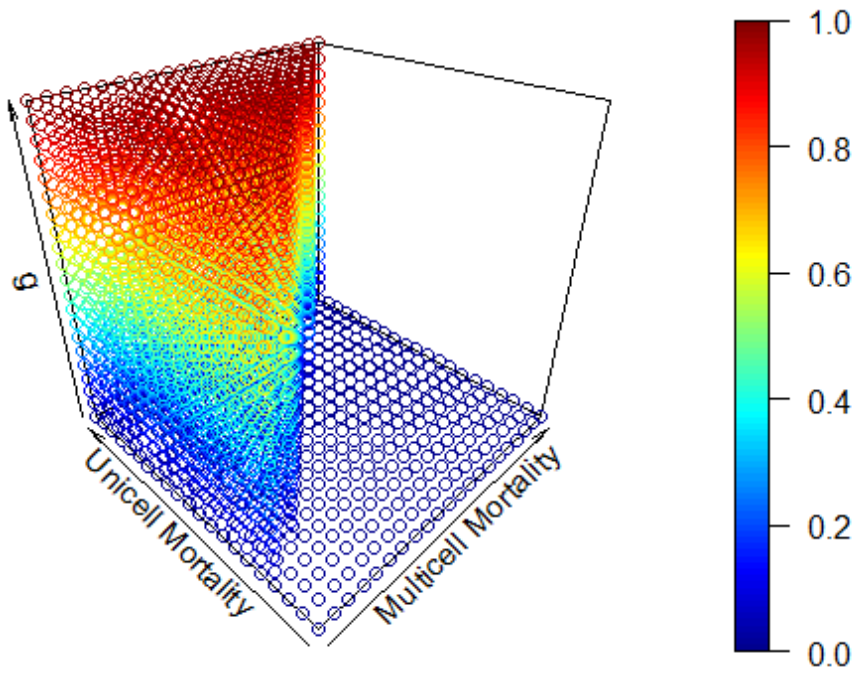

Figure 5: All *g* values, probability of branching into the multicellular class, associated with uni- and multicellular mortality. When multicell mortality is higher than unicellular mortality only a single *g* value, $g = 0$, is associated with the maximum population growth rate.

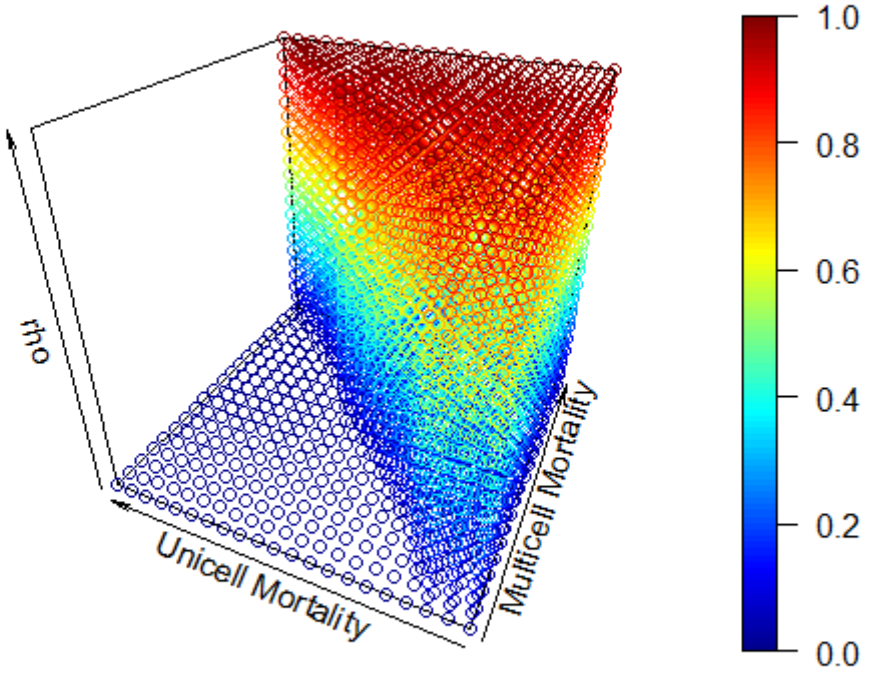

Figure 6: All ρ values, probability of branching into the multicellular class, across all values of uni- and multicellular mortality associated with the maximum population growth rate.

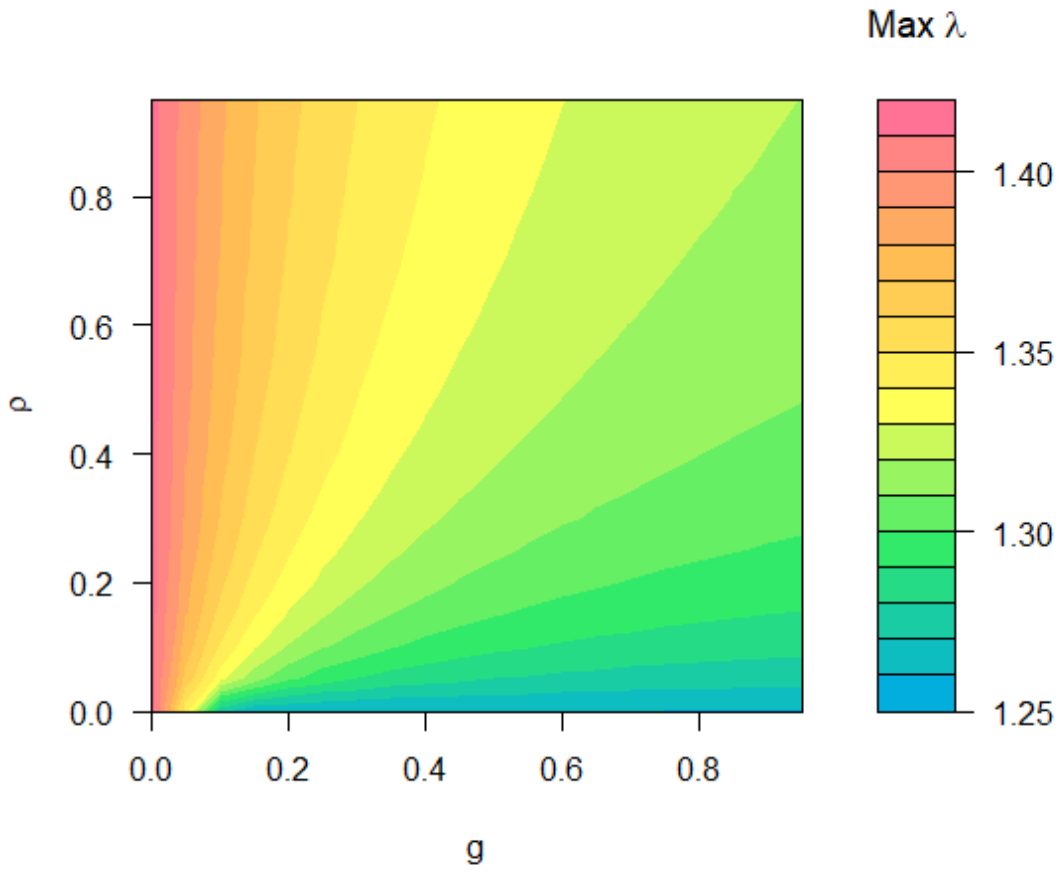

Figure 7: Maximum population growth rates (λ) under the tradeoff that specifies $R_1 > R_2$. Here $R_1 = \sqrt{2}$, $R_2 = \sqrt[3]{2}$, and $m_1 = 0.2928932$, so that $r_1 = 2$, $b = 0.35$, $c = 0.05648173$, $r_2 = 1.65$, and $m_2 = 0.2364115$. Warmer colors represent higher asymptotic growth rates; cooler colors represent lower growth rates

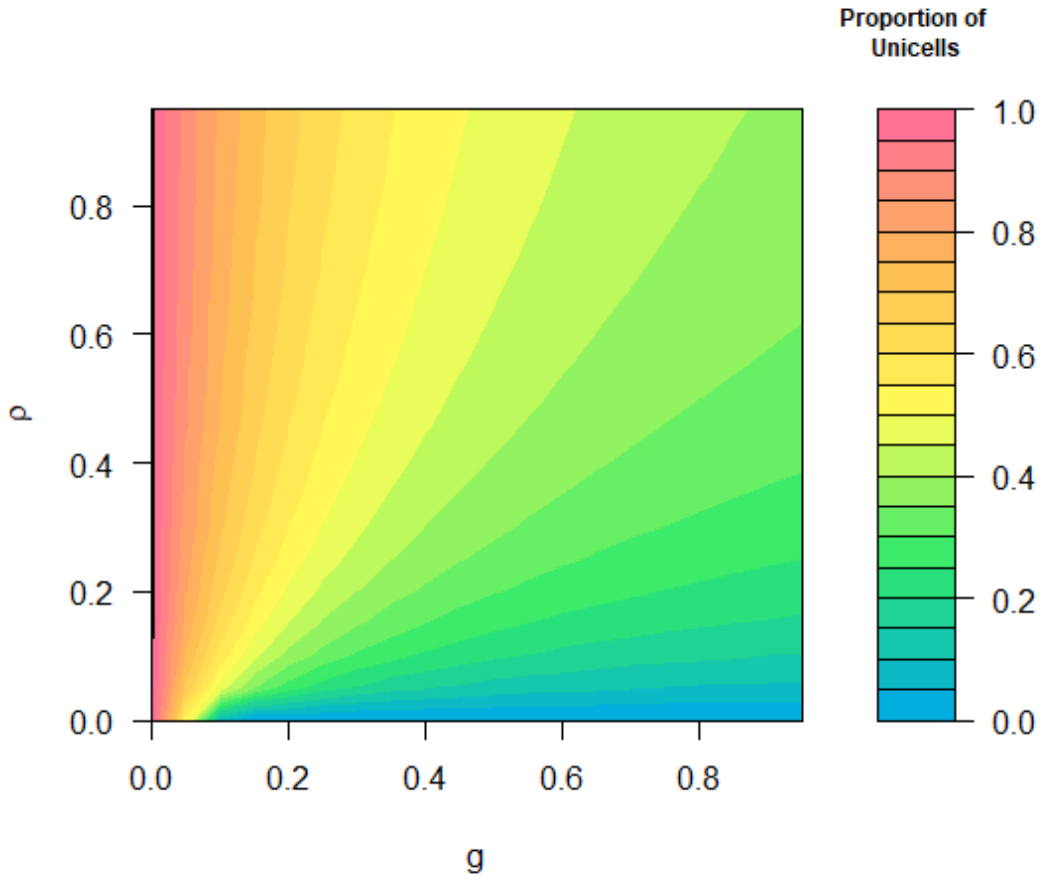

Figure 8: Proportion of unicellular individuals associated with the maximum growth rate (λ) under the tradeoff that specifies $R_1 > R_2$. Here $R_1 = \sqrt{2}$, $R_2 = \sqrt[3]{2}$, and m_1=*0.2928932*, resulting in r_1 = *2*, b = *0.35*, c = *0.05648173*, r_2 =*1.65*, and m_2 = *0.2364115*. Warmer colors represent higher proportions of unicellular individuals; cooler colors represent a higher proportion of multicellular individuals.

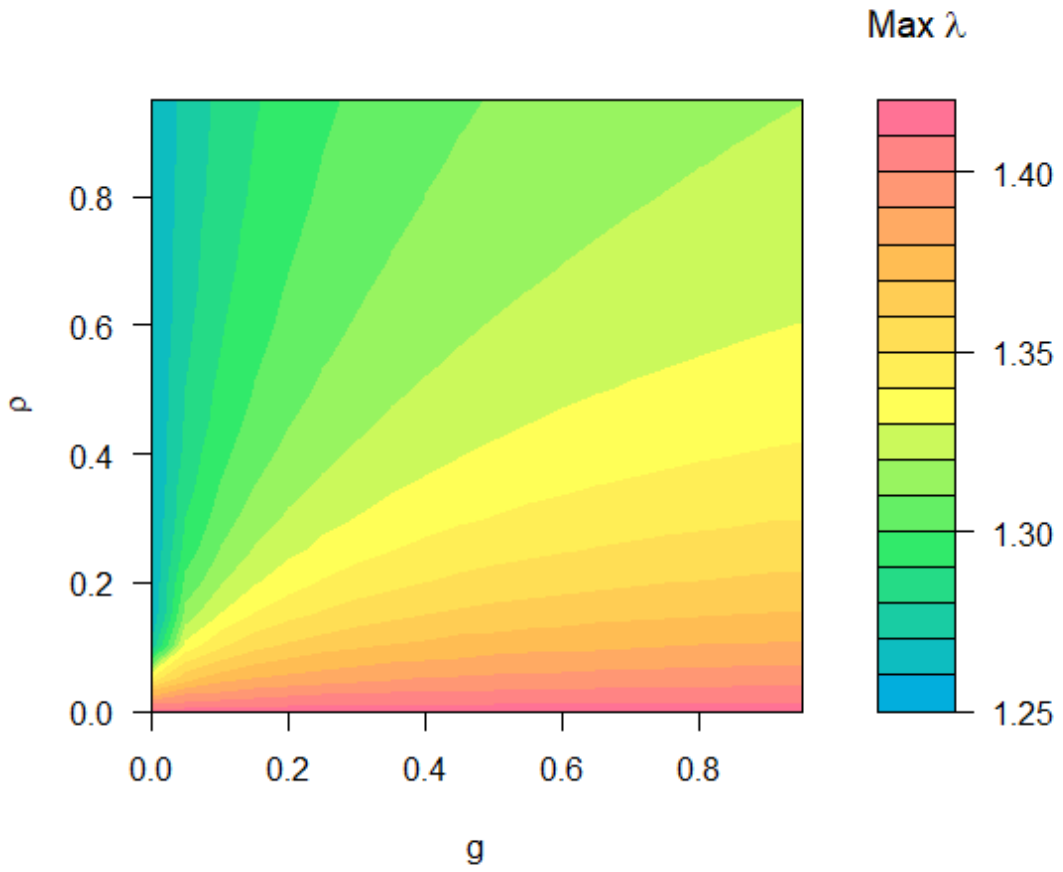

Figure 9: Maximum population growth rates (λ) under the tradeoff that specifies $R_1 < R_2$. Here $R_1 = \sqrt[3]{2}$, $R_2 = \sqrt{2}$, and $m_1 = 0.2$, so *that* $r_1 = 2$, $b = 0.35$, $c = 0.2271386$, $r_2 = 1.65$, and $m_2 = 0.1429009$. Warmer colors represent higher population growth rates.

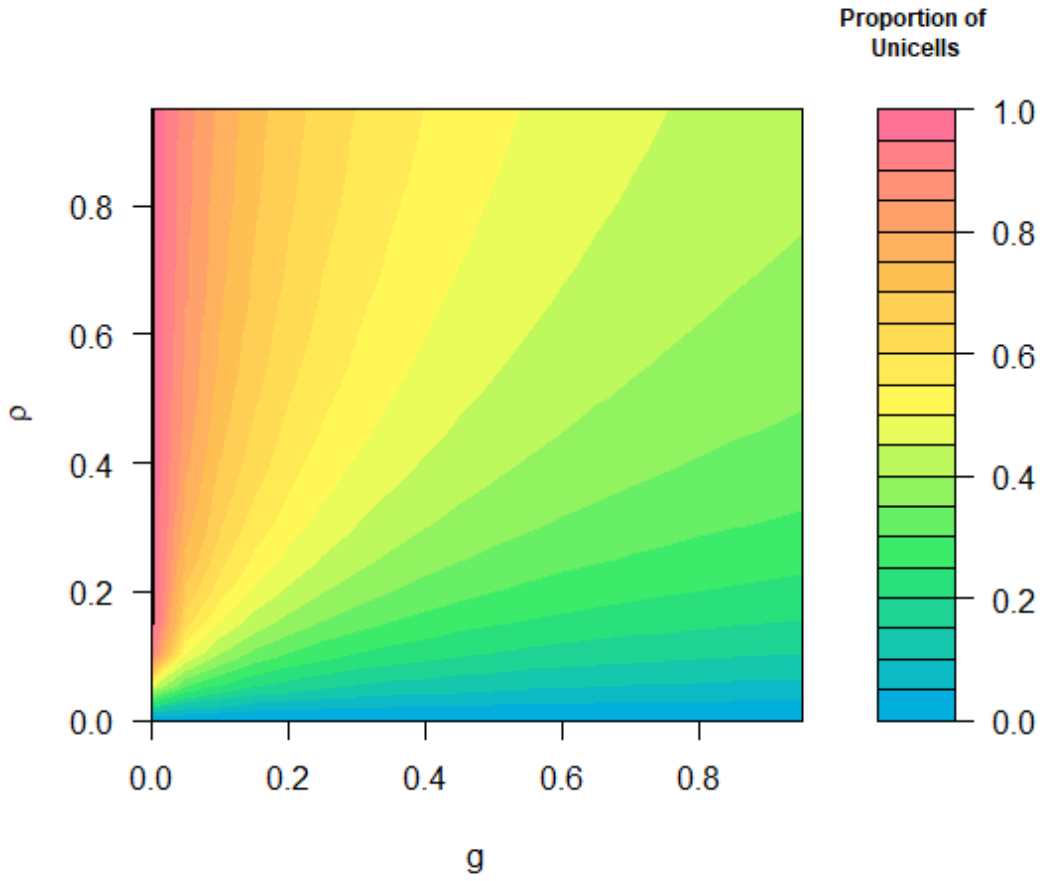

Figure 10: Proportion of unicellular individuals associated with the maximum growth rate (λ) under the tradeoff that specifies $R_1 < R_2$. *Here* $R_1 = \sqrt[3]{2}$, $R_2 = \sqrt{2}$, and m_1*=0.2*, so that r_1 *= 2*, b *= 0.35*, c *= 0.2271386*, r_2 *=1.65*, and m_2*= 0.1429009*. Warmer colors represent higher proportions of unicellular individuals; cooler colors represent a higher proportion of multicellular individuals

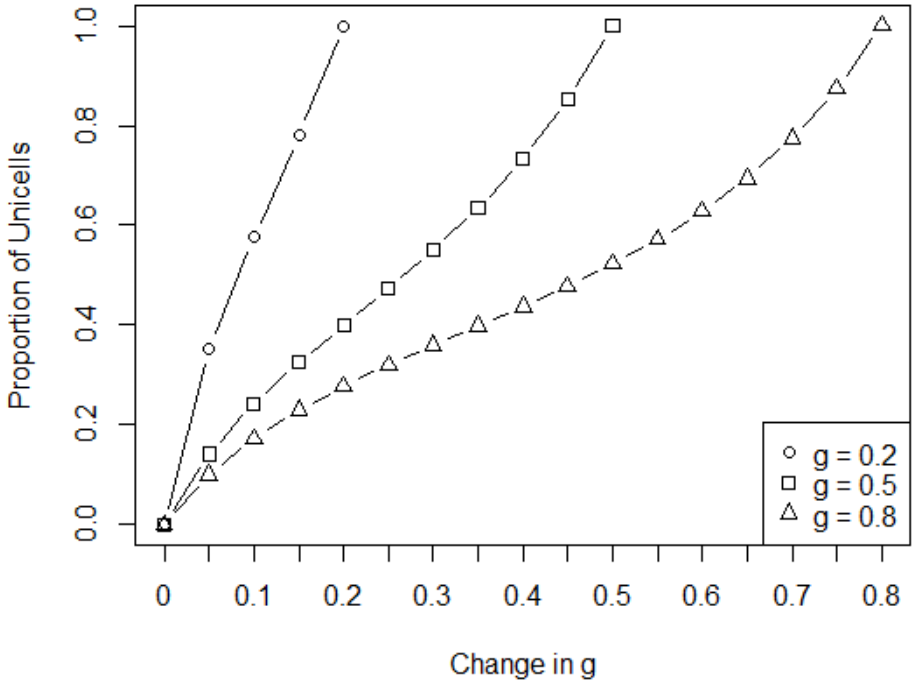

Figure 11: Rate of selection for a unicellular population for multiple values of g when $R_1 > R_2$. The lines represent both the proportion of unicells and the maximum population growth rate. Using the minimum population growth rate associated with a specified initial value of g, the selection gradient follows the steepest curve to the next highest potential growth rate. The shallower gradient for larger initial g values corresponds to areas of parameter space where more itinerant life history strategies are exhibited.

CHAPTER 5

DISCUSSION AND CONCLUSIONS

Several broad trends emerge from my analysis of the model. The endpoints for maximum and minimum population growth rates are defined by the class-specific growth rates. Extending from this, the highest possible growth rate will be equivalent to either R_1 or R_2 and the associated population will consist of individuals exhibiting the morphology corresponding to the highest per class aggregate growth rate. Given this, if selection is acting to increase the maximum growth rate the class exhibiting the larger aggregate growth rate will eventually exclude individuals with the other morphology.

While the maximum and minimum growth rates in each case are associated with monomorphic populations, for intermediate growth rates this relationship is more complex. When both g and ρ are greater than zero but less than one, the same growth rate may be achieved with varying proportions of unicellular and multicellular individuals and likewise a given proportion of unicellular to multicellular individuals may be associated with multiple growth rates. Because the growth rates do not map perfectly onto specific size structure combinations, this indicates that changes in life history will have different effects on both the whole population growth rate and size structure contingent on current values of g and ρ. As seen in Figure 11, the selection gradient may vary greatly depending on where a population is initially located in g-ρ space. If selection acts to increase the maximum population growth rate, then given an initial set of probabilities I can predict the life history strategy which should be favored under a specified tradeoff. When $R_1 > R_2$, g should be minimized so that individuals never leave the unicellular

form. Likewise, When $R_2 > R_1$, ρ should be minimized. In both cases I expect the class with the larger aggregate growth rate to replace the class with the smaller growth rate. When only a single class is present the cost associated with the alternate morphology will be high meaning the alternate morphology should appear only rarely and may eventually be excluded from the reproductive population.

At higher values of both g and ρ, for example $g > 0.75$ and $\rho > 0.75$, it takes larger changes in g and ρ to increase the population growth rate, suggesting a shallower selection gradient for all tradeoff scenarios. There is potential for the population growth rate and size structure to remain relatively stationary in this region even as life history changes a lot. A change in environmental conditions may push the population out of this high g and ρ area so that a change in the intensity and direction of selection may occur. For example, if nutrients become limiting the unicellular form may become increasingly advantageous due to more efficient uptake. This should select for increasingly small values of g.

Because g and ρ are non-independent changing environmental conditions may alter the value of the parameter not under direct selection. For instance, if selection is reducing g from an initial value of $g = 0.2$, once the population has evolved to g = 0 the corresponding ρ will be $\rho = 0.2$, however if sudden environmental shifts change the rate of selection, such a decrease in nutrient availability, then it is plausible that the ρ value at $g = 0$ may be higher or lower than expected under a constant nutrient environment. This has limited importance if conditions remain constant but may be relevant if nutrient availability or predation intensity changes to favor the alternate class.

I used this model to examine a single morphological difference, however many organisms exhibit more than two morphological forms over their lifespan. This model could be

modified to incorporate more complex tradeoffs between classes, additional classes, or may even be converted into a model of ontogenic development across multiple stages. These may reveal other important tradeoffs that dictate asymptotic growth rates and population size structure. For instance, experiments into the evolution of multicellularity suggest that initial variation in the number of cells within a colony may be high, but that this variance may decrease over several generations (Boraas, et al., 1998). This finding suggests that colony fitness may be dependent on developing an optimal number of cells; with the incorporation of additional size classes or more nuanced relationships between classes I may be able to determine the optimal cell number for a theoretical multicellular species.

As with any theoretical study the ability to empirically study the model is beneficial for confirming and supporting model predictions. This particular model lends itself well to study in aquatic micro or mesocosms as many of the organisms which inspired this analysis are phytoplankton which exhibit both unicellular and multicellular body forms depending upon environmental conditions. Microcosms containing producers, such as *Chlamydomonas reinhardtii* or *Chlorella vulgaris*, and their predators have already shown that larger multicellular organisms emerge in the presence of predators, however many of these studies examined the competitive ability of multiple clonal lines rather than the potential for adaptation within a single clonal population as this model does (Yoshida, et al., 2003; Ellner & Becks, 2011).

One limitation of this model is that both the nutrient and predation environments are constant over time. As rapidly changing environmental conditions can alter both the speed and direction of selection within a population the weight of any specific tradeoff between growth and mortality may be increased or decreased when the environment changes. Being able to better understand and incorporate the rate of evolutionary or plastic change within a population may allow for

better predictions about long term population dynamics in response to climate change and anthropogenic drivers of such change.

REFERENCES

Arnold, W. S., 1984. The effects of prey size, predator size, and sediment composition on the rate of predation of the blue crab Callinectes sapidus Rathbun on the hard clam Mercenaria mercenaria (Linne). *Journal of Experimental Marine Biology and Ecology*, Volume 80, pp. 207-219.

Bassar, R. D. et al., 2010. Local adaptation in Trinidadian guppies alters ecosystem processes. *Proceedings of the National Academy of Sciences,* 107(8), pp. 3616-3621.

Becks, L., Ellner, S. P., Jones, J. & Hairston, N. J., 2010. Reduction of adaptive genetic diversity radically alters eco-evolutionary comunity dynamics. *Ecology Letters,* Volume 13, pp. 989-997.

Boraas, M. E., Seale, D. B. & Boxhorn, J. E., 1998. Phagotrophy by a flagellare selects for colonial prey: A possible origin for multicellularity. *Evolutionary Ecology,* Volume 12, pp. 153-164.

Brooks, J. L. & Dodson, S. I., 1965. Predation, Body Size, and Composition of Plankton. *Science,* 150(3692), pp. 28-35.

Caswell, H., 2001. *Matrix Population Models.* s.l.:John Wiley & Sons, Ltd..

Charnov, E. L., 1991. Evolution of life history variation among female mammals. *Proceedings of the National Academy of Sciences,* Volume 88, pp. 1134-1137.

Charnov, E. L., 1993. *LIfe History Invariants.* Ocford: Oxford University Press.
Cole, L. C., 1954. Population consequences of life history phenomena. *The Quarterly Review of Biology,* 29(2), pp. 103-137.

Cuadrado, M. & Loman, J., 1999. The Effects of Age and Size on Reproductive Timing in Female Chamaeleo chamaeleon. *Journal of Herpetology,* 33(1), pp. 6-11.

deRoos, A. & Persson, L., 2013. *Population and Community Ecology of Ontogenic Development.* Princeton: Princeton University Press.

Ellner, S. P. & Becks, L., 2011. Rapid prey evolution and the dynamics of two-predator food webs. *Theoretical Ecology,* Volume 4, pp. 133-152.

Eppley, R. W. & Thomas, W. H., 1969. Comparison of Half-Saturation For Growth and Nitrate Uptake of Marine Phytoplankton. *Journal of Phycology,* Volume 5, pp. 375-379.

Fischer, B. B. et al., 2014. Phenotypic plasticity influeces the eco-evolutionary dynamics of a predator-prey system. *Ecology,* 95(11), pp. 3080-3092.

Hein, M., Pederson, M. F. & Sand-Jensen, K., 1995. Size-dependent nitrogen uptake in micro- and macroalgae. *Marine Ecology Progress Series,* Volume 118, pp. 247-253.

Hutchinson, G. E., 1959. Homage to Santa Rosalia or why are there so many kinds of animals?. *The American Naturalist,* 93(870), pp. 145-159.

Irwin, A. J., Finkel, Z. V., Schofield, O. M. & Falkowski, P. G., 2006. Scaling up from nutrient physiology to the size-structure of phytoplankton communities. *Journal of Plankton Research,* 28(5), pp. 459-471.

Iwasa, K. & Murakami, S., 1968. Palmelloid Formation of Chlamydomonas I. Palmelloid Induction by Organic Acids. *Physiologia Plantarum,* Volume 21, pp. 1224-1233.

Jenkins, D. G. et al., 2007. Does size matter for dispersal distance?. *Global Ecology and Biogeography,* Volume 16, pp. 415-425.

Kempes, C. P., Dutkiewicz, S. & Follows, M. J., 2012. Growth, metabolic partitioning, and the size of microorganisms. *Proceedings of the National Academy of Sciences,* 109(2), pp. 495-500.

Lurling, M. & Beekman, W., 2006. Palmelloids formation in Chlamydomonas reinhardtii: defense against rotifer predators?. *Annales de Limnologie-International Journal of Limnology,* 42(2), pp. 65-72.

Michod, R. E., 2005. On the transfer of fitness from the cell to the multicellular. *Biology and Philosophy,* Volume 20, pp. 967-987.

Nilsson, P. A. & Bronmark, C., 2000. Prey vulnerability to a gape-size limited predator: behavioural and morphological impacts on northern pike piscivory. *Oikos,* Volume 88, pp. 539-546.

Pastorok, R. A., 1981. Prey Vulnerability and Size Selection by Chaoborus Larvae. *Ecology,* 62(5), pp. 1311-1324.

Pawar, S., Dell, A. I. & Savage, V. M., 2012. Dimensionality of consumer search space drives trophic interaction strength. *Nature,* Volume 486, pp. 485-489.

Ratcliff, W. C., Denison, R. F., Borrello, M. & Travisano, M., 2012. Experimental evolution of multicellularity. *Proceedings of the National Academy of Sciences,* 109(5), pp. 1595-1600.

Reznick, D. & Endler, J. A., 1982. The Impact of Predation on Life History Evolution in Trinidadian Guppies (POECILIA RETICULATA). *Evolution,* 36(1), pp. 160-177.

Roughgarden, J. & Fuentes, E., 1977. The environmental determinants of size in solitary populations of West Indian Anolis lizards. *Oikos,* Volume 29, pp. 44-51.

Ryther, J. H., 1969. Photosynthesis and Fish Production in the Sea. *Science,* 166(3901), pp. 72-76.

Sala, E. & Zabala, M., 1996. Fish predation and the structure of the sea urchin Paracentrotus lividus populations in the NW Mediterranean. *Marine Ecology Progress Series,* Volume 140, pp. 71-81.

Stanley, S. M., 1973. An Ecological Theory for the Sudden Origin of Multicellular Life in the. *Proceedings of the National Academy of Sciences,* 70(5), pp. 1486-1489.

Yoshida, T. et al., 2003. Rapid evolution drives ecological dynamics in a predator-prey system. *Nature,* Volume 424, pp. 303-306.